2012 IEEE/RSJ International Conference on
Intelligent Robots and Systems
October 7-12, 2012. Vilamoura, Algarve, Portugal

Controller Performance of Marine Robots in Reminiscent Oil Surveys

Shayok Mukhopadhyay, Chuanfeng Wang, Steven Bradshaw, Valerie Bazie, Sean Maxon, Lisa Hicks, Mark Patterson and Fumin Zhang

***Abstract*— A class of path following and formation controllers are implemented on marine robots performing autonomous surveys in regions polluted by crude oil during the Deepwater Horizon oil spill. The controllers enable the robots to follow lines and curves, and maintain formation collectively while measuring reminiscent crude oil along their paths. The controllers are mathematically sound with proven convergence and robustness. However, their performance in the surveying missions is affected by natural disturbances caused by wind and water currents, and constraints such as sensor inaccuracy, localization errors, and network delays. This paper evaluates the performance of our controllers based on data collected during a survey performed at Grand Isle, Louisiana. These results will provide guidance for mission designs and inspire the future developments of our marine robots used to perform autonomous environmental surveys.**

I. INTRODUCTION

Marine surveys are crucial for assessing risks of maritime disasters such as the Deepwater Horizon oil spill which occurred in 2010. After the event a report was submitted to the U.S. President in January 2011 [1] with recommendations for creating the technology and tools needed to effectively handle such catastrophes in future. Autonomous surveys are especially attractive in marine environments that are less than ideal for human based methods.

Autonomous surveys using marine vehicles require path planning and path following for which previous results exist [2]–[6]. Marine vehicles are usually underactuated, making this a challenging control problem. Using a swarm of robots can increase the efficiency or accuracy of a survey [7], [8]. Although the theory in this field is sufficiently advanced [9], [10] only few theoretical results have been evaluated in field tests [11]. A class of curve tracking controllers based on the Frenet-Serret framework has been developed previously [12] and has seen satisfactory performance on mobile robots and ocean gliders [13], [14]. The robustness of these control laws have been recently justified [10] and agree with observations made on field. Therefore, it is worthwhile to evaluate the controllers on marine robots developed for oil spill surveys, where the robots, the environment, and the technical challenges differ significantly from previous experiments using mobile robots and ocean gliders.

One year after the Deepwater Horizon oil spill, we performed a survey in Grand Isle, Louisiana as heavy pollution was reported here during the oil spill. Our fleet of marine robots collected data to evaluate the level of oil remaining after large scale cleanup operations. This paper reports experimental results related to controller performance of two marine robots employed in the survey. The first robot is the Victoria class autonomous surface vessel (ASV-Victoria) developed and built by a student team named Georgia Tech Savannah Robotics (GTSR) formed by the authors from Georgia Tech. ASV-Victoria shares a similar twin-hull catamaran design with other ASVs like the DELFIM, SESAMO, and ROAZ [15]–[18] which are mechanically robust for sea conditions. The second robot is a Fetch class autonomous underwater vehicle (AUV-Fetch) developed by Prof. Mark Patterson at the College of William and Mary. AUV-Fetch is a commercial-quality versatile marine robot that can be used either as a surface vessel or as an underwater vehicle. These robots are illustrated in Fig. 1.

We present experimental results on parameter identification, path following control, and formation control for the two marine robots. Controller performance was affected by natural disturbances like winds and current, and limitations like sensor inaccuracy, localization error and communication delays. Technical errors and faults also cause large deviations from theoretical predictions. Nevertheless, the experimental results show that the control laws are robust to disturbances and faults.

The paper is organized as follows. In section II we describe the hardware and software systems for each vehicle. The algorithms and control laws used are presented in section III, followed by the experiments and our conclusions in sections IV and V respectively.

II. THE MARINE ROBOTS

A. ASV-Victoria

1) Hardware: ASV-Victoria shown in the upper half of Fig. 1 is developed and built by GTSR. It weighs 50 kilograms. It is 100 cm in length and 75 cm wide. The trim is approximately 50 cm with the overall height being about 75 cm. Victoria's hulls are composed of multiple layers of fiberglass sheets. On board electronics, propulsion and power systems are arranged to keep the center of mass closest to the center of the boat to minimize pitching.

The vehicle can be remotely controlled within a range of approximately 500 meters. Its thrusters are capable of

Shayok Mukhopadhyay, Steven Bradshaw, Valerie Bazie, Sean Maxon, Lisa Hicks and Fumin Zhang are with the School of Electrical and Computer Engineering, Georgia Institute of Technology, Atlanta, GA 30322, USA. Emails: shayok, sbradshaw6, vbazie3, sean.maxon, lhicks7, fumin@gatech.edu.

Chuanfeng Wang is with the School of Mechanical Engineering, Georgia Institute of Technology, Atlanta, GA 30322, USA. Email: cwang329@gatech.edu

Mark Patterson is with the Virginia Institute of Marine Science, The College of William and Mary, Gloucester Point, Virginia 23062, USA. Email: mrp@vims.edu

978-1-4673-1735-1/12/S31.00 ©2012 IEEE

Fig. 1. GTSR's ASV Victoria and the VIMS AUV Fetch 1

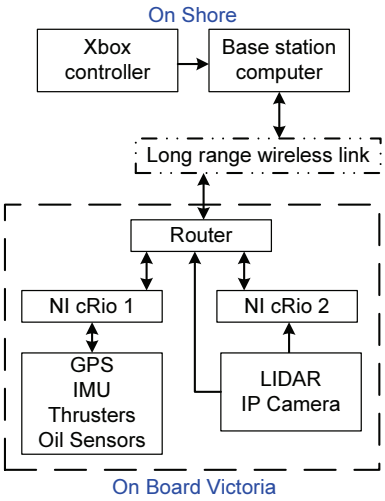

Fig. 2. A high level schematic of Victoria's electrical systems

producing up to 60 pounds of thrust, resulting in a maximum speed of 2 m/s. An inertial motion unit, an ethernet camera, oil sensors and a GPS receiver are the main sensors onboard Victoria. The main computational units are National Instruments (NI) Compact RIOs (cRIO) which are modular and combine an embedded real-time processor, a field programmable gate array (FPGA), and I/O modules. Fig. 2 shows a high level view of Victoria's electrical systems. Two NI-cRIO's are used onboard Victoria. One handles lower level thruster control and data acquisition where as the other one handles the navigation/vision system. Victoria also houses three isolated power systems.

2) Software: National Instruments (NI) LabVIEW is used onboard ASV-Victoria. The software architecture in Fig. 3 shows four main virtual instruments (VI's): Main PC, Main RIO, Main FPGA and Cooperative Control. Main RIO and

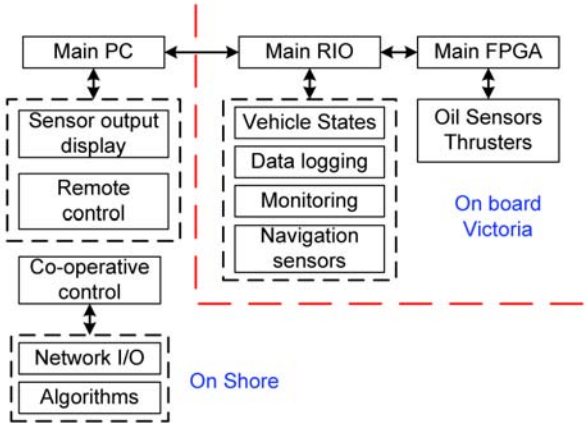

Fig. 3. A high level schematic of Victoria's software architecture

Main FPGA run on a cRIO; Main PC and Cooperative Control run on the control laptop. The Cooperative Control VI queries a different vehicle for its orientation angle and position and sends appropriate commands enabling it to track lines or curves. All inter-vehicle communication happens over a Wi-Fi network. This architecture makes a survey fleet scalable as any number of nodes can be added as masters to control other slave vehicles.

B. AUV Fetch-1

1) Hardware: The Fetch 1 is an autonomous underwater vehicle (AUV) developed by professor Mark Patterson of the College of William and Mary. It served as an ASV for some experiments performed during our survey. The Fetch 1 has an aluminum hull, is 6.5 feet long, weighs 220 pounds, and is rated to a maximum diving depth of 500 feet. It is driven by a single propeller and steered with two pairs of single-degree-of-freedom control surfaces. Fetch 1 is outfitted with Wi-Fi as well as a FreeWave RF serial modem that maintains constant contact with a shore station as long as the vehicle is on the surface. The Fetch 1 used an assortment of sensors including GPS, water temperature and salinity sensors, as well as a crude oil sensor.

2) Software: Fetch 1's main flight computer runs LabVIEW. We controlled Fetch 1 via its teleoperation mode from a commanding computer. Commands were sent to Fetch via Victoria's shoreside control computer or the cRIO onboard Victoria itself depending on mode of operation. Feedback control algorithms operated at a frequency of 0.5 Hz, with data exchange taking place once every two seconds.

C. Mathematical models for the vehicles

We used the simple and widely used unicycle model to describe the dynamics of Victoria and Fetch 1 as point particles. Let x, y represent the position of a robot. The linear and angular velocities v, ω of ASV-Victoria can be written in terms of velocities of the left and the right thrusters (v_l, v_r) as $v = \frac{v_l+v_r}{2}$, $\omega = \frac{v_r-v_l}{2l}$, $v_l = K_1 n_l$ and $v_r = K_2 n_r$ where l is the distance between the horizontal axis of the vehicle and the horizontal axes passing through the centers

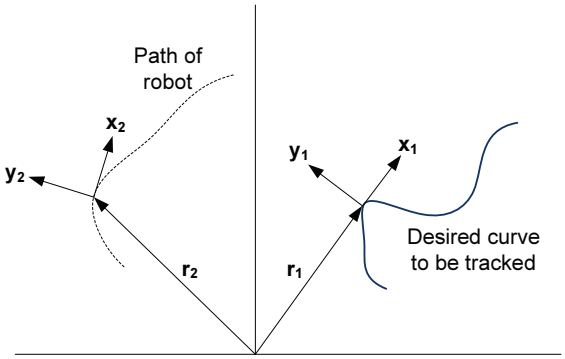

Fig. 4. Curve tracking using two Frenet-Serret frames

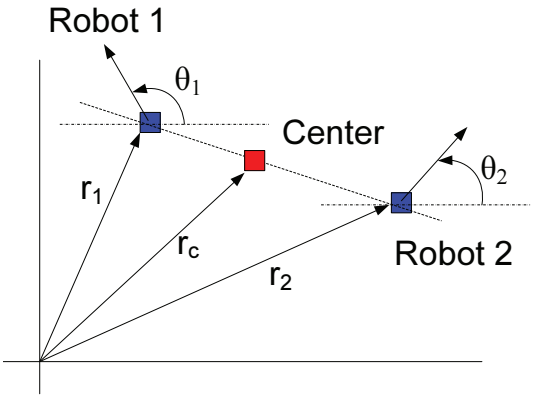

Fig. 5. Formation control

of each thruster. The quantities n_l, n_r represent the duty cycles of the signals sent to the left and right thrusters respectively. The constants K_1, K_2 relate the duty cycles to the velocities v_l, v_r. Substituting these back into the unicycle model provides a model which accounts for the thruster coefficients K_1, K_2. We have developed simple algorithms to estimate the parameters K_1 and K_2 from experimental data.

III. Algorithms and Control Laws

A. Parameter extraction

The parameters K_1 and K_2 can be obtained from measurements as $K_1 = \frac{v-l\omega}{n_l}$, $K_2 = \frac{v+l\omega}{n_r}$. Open loop tests are performed to identify these parameters. In the open loop tests, the thruster commands n_r, n_l stay constant for a particular test. The actual values of v, ω can be estimated from the GPS data and used to calculate K_1 and K_2.

B. Curve tracking

We formulate the curve tracking problem using Frenet-Serret equations as in [12]. Fig. 4 shows two particles. Let $\mathbf{r}_2$ denote the position vector of the robot and $\mathbf{r}_1$ denote the position of a point closest to the robot along a curve which the robot is trying to track.

Further define the vector $\mathbf{r} = \mathbf{r}_2 - \mathbf{r}_1$ and $\rho = \|\mathbf{r}\|$ (the relative distance). We also define ϕ as the relative bearing between the tangent vectors $\mathbf{x}_1$ and $\mathbf{x}_2$. The variables (ρ, ϕ) are called the shape variables. Taking the time derivative of the shape variables we get the following dynamics.

$$\dot{\rho} = -\sin\phi \tag{1}$$

$$\dot{\phi} = \left(\frac{k_1}{1+k_1\rho}\right)\cos\phi - u_2 \tag{2}$$

In the above equations u_2 is the steering command for the robot. The following control law enables us to perform curve tracking.

$$u_2 = \left(\frac{\pm k_1}{1+k_1\rho}\right)\cos\phi \pm K_p(\rho-\rho_0)\cos\phi + \mu\sin\phi \tag{3}$$

The "$\pm$" signs in the above law are used depending on whether the initial position of the robot is to the left or the right of the curve. The desired separation between the robot and the curve is specified by ρ_0 in eqn. (3). The controller in equation (3) resembles a PD controller, where K_p, μ can be viewed as the proportional and derivative gains respectively. In eqn. (3) k_1 represents the algebraic curvature of the curve being tracked. For details readers should consult [12].

C. Formation control

A vehicle can be viewed as a Newtonian particle with unit mass that obeys $\ddot{\mathbf{r}} = \mathbf{f}$, where $\mathbf{f}$ is a real vector with two rows and one column. $(\mathbf{r}, \dot{\mathbf{r}})$ forms the state of the particle. The Newtonian particle model is more convenient to use for formation control [19], [20]. As is shown in [13], [21], the Newtonian particle model is equivalent to the Frenet-Serret equations in describing the motion of the vehicles. We can define a unit vector $\mathbf{x} = \dot{\mathbf{r}}/\|\dot{\mathbf{r}}\|$ as long as $\dot{\mathbf{r}}$ is not zero. We also define the vector $\mathbf{y}$ as follows.

$$\mathbf{y} = \begin{bmatrix} 0 & -1 \\ 1 & 0 \end{bmatrix}\mathbf{x} \tag{4}$$

For formation control we use the Jacobi transform to decouple the shape and orientation dynamics from the dynamics of the formation center [8], [19], [20]. Fig. 5 shows two robots represented by vectors $\mathbf{r}_1$ and $\mathbf{r}_2$ and their center by $\mathbf{r}_c$. The respective forces for these particles are given by $\mathbf{f}_1, \mathbf{f}_2$, and $\mathbf{f}_c$. The Jacobi vector $\mathbf{q}_1$ for this system is given by $\mathbf{q}_1 = \frac{1}{2}(\mathbf{r}_2 - \mathbf{r}_1)$, and the formation center $\mathbf{r}_c = \frac{1}{2}(\mathbf{r}_1 + \mathbf{r}_2)$. From the Newtonian particle model we can now write the following equations.

$$\ddot{\mathbf{r}} = \mathbf{f}_c = \frac{1}{2}(\mathbf{f}_1 + \mathbf{f}_2) \tag{5}$$

$$\ddot{\mathbf{q}}_1 = \mathbf{u}_1 = \sqrt{2}(\mathbf{f}_2 - \mathbf{f}_1) \tag{6}$$

In the above equations, the dynamics for the center have been separated from the dynamics for formation control. Now we separately design the input $\mathbf{u}_1$ for formation control and the force $\mathbf{f}_c$ for making the center of the formation track a curve. This achieves curve tracking using multiple vehicles while staying in formation. The force that will be applied to the center is $\mathbf{f}_c = \|\dot{\mathbf{r}}_c\|^2 u_c \mathbf{y}_c$ where u_c is designed using equation (3). For formation control, we define the desired shape by vector $\mathbf{q}_0$. Formation control is achieved by using

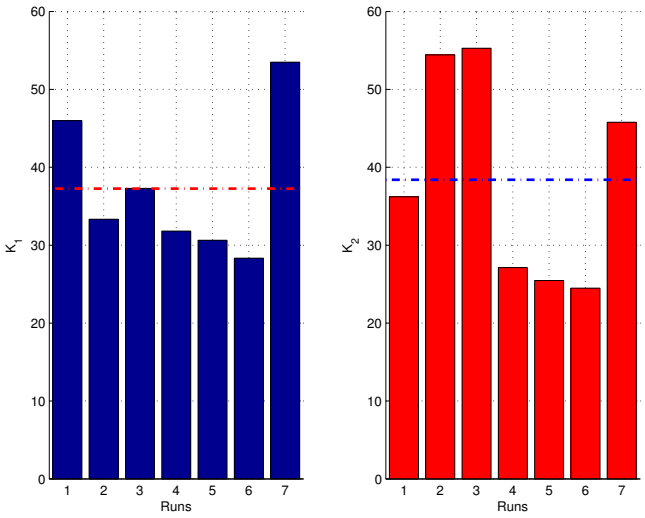

Fig. 6. Estimating the parameters K_1 and K_2

a simple PD controller as follows, $\mathbf{u}_1 = -K_{pf}(\mathbf{q}_1 - \mathbf{q}_0) - K_{df}\dot{\mathbf{q}}_1$. From $\mathbf{f}_c$ and $\mathbf{u}_1$ we calculate the individual forces $\mathbf{f}_1$, $\mathbf{f}_2$ and the individual linear and angular velocity commands γ_k, v_k for each vehicle as follows:

$$\mathbf{f}_1 = \mathbf{f}_c - \frac{1}{2\sqrt{2}}\mathbf{u}_1,\ \mathbf{f}_2 = \mathbf{f}_c + \frac{1}{2\sqrt{2}}\mathbf{u}_1 \tag{7}$$

$$\gamma_1 = \mathbf{f}_1 \cdot \mathbf{x}_1,\ \gamma_2 = \mathbf{f}_2 \cdot \mathbf{x}_2 \tag{8}$$

$$\dot{v}_k = \gamma_k,\ \omega_k = \frac{\mathbf{f}_k \cdot \mathbf{y}_k}{v_k},\ k = 1, 2. \tag{9}$$

IV. Experiments

The experimental results presented in this paper are from a 21 day survey performed at the Grand Isle, Louisiana where crude oil has been spotted [1] along the beaches. The experiments were carried out in a tidal lagoon in the Grand Isle State Park using ASV Victoria and AUV Fetch 1. First we present the results for parameter identification. Then we test line and curve following control for individual robots. Finally we report the results of a trial on formation control. Note that during most experimental runs, the currents measured in the lagoon were approximately 20 cm/s pointing Northeast and wind speeds varied between 5 and 10 mph. Readers can view ASV-Victoria and Fetch 1 performing curve tracking runs in the video accompanying this paper.

A. Parameter indentification

For parameter extraction we operate ASV-Vicoria in the open loop mode and send seven sets of thruster speeds to the lower level thruster controllers. Fig. 6 shows the values obtained for the constants K_1 and K_2 calculated as shown in section III-A for each of the seven open loop tests performed. The dotted lines show the average values obtained for these parameters which are $K_1 = 37.26$ and $K_2 = 38.4$.

B. Path following

Fig. 7 shows the results of a line following run with ASV Victoria. The dotted line is the reference line the ASV is

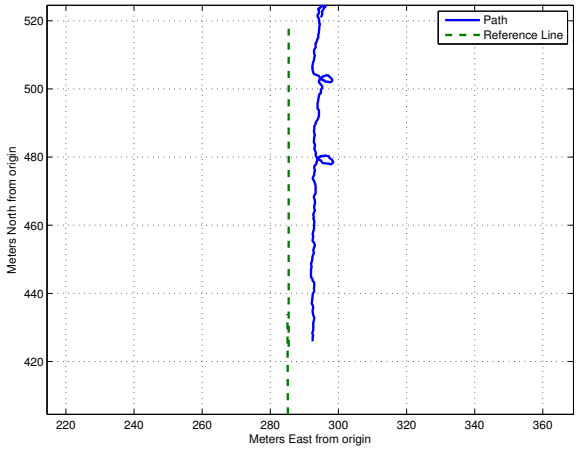

Fig. 7. Line following using ASV Victoria

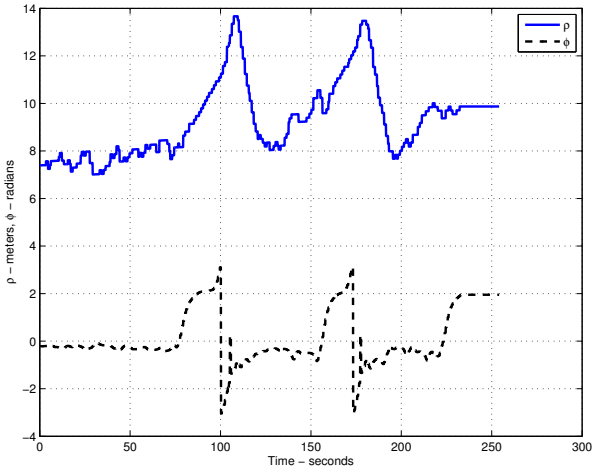

Fig. 8. Error analysis for line following using ASV Victoria

trying to follow. The solid curve shows the path taken by the ASV. The control gains for this run are: $\mu = 5$, $K_p = 1$, and the desired buffer between the line and the vehicle i.e. ρ_0 is set to 6. The ASV follows the line well but it has some intermittent large deviations. This is shown in detail in Fig. 8, where the solid line represents the distance error ρ and the dotted line represents the error in orientation ϕ.

From Fig. 8 we see that ϕ stays close to zero. Even if disturbances occur, ϕ is seen to come back to zero reasonably quick. The distance error ρ is maintained just above 8 on an average. Corresponding to the two loops in the path of the ASV seen in figure 7 we find disturbances in ρ and ϕ in Fig. 8. From analyzing the data it appears that those disturbances occur due to faults occurring in the electronic speed controllers on the thrusters. However, it is seen that the control law is robust enough as it recovers from the disturbance and the vehicle converges back to following the line again.

Fig. 9 shows the result of tracking a circular path using ASV Victoria, overlayed on a Google map. From figure 9 the

Fig. 9. Tracking a circular curve using ASV Victoria

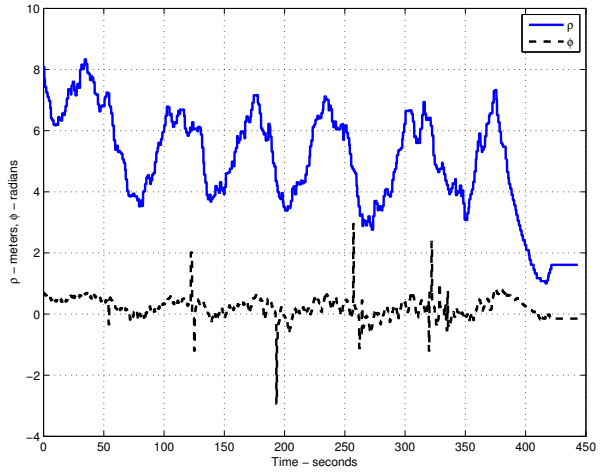

Fig. 10. Error analysis for curve tracking using ASV Victoria

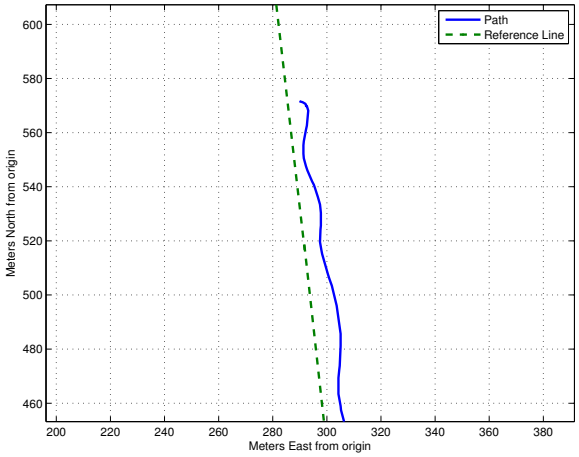

Fig. 11. Line following using Fetch 1

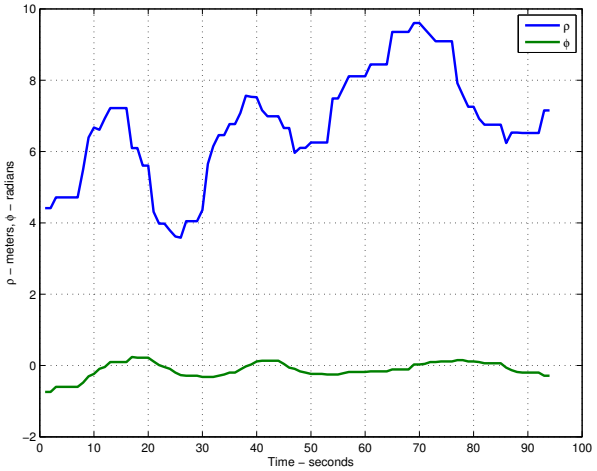

Fig. 12. Error analysis for line following using Fetch 1

circle appears displaced as the vehicle is affected by currents (south west to north east) forcing it to the right. For the path shown in Fig. 9, the control gains are $\mu = 5$, $K_p = 1$, the buffer is $\rho_0 = 4m$, the radius of the circle $R = 1m$ and the direction of motion is clockwise.

Fig. 10 shows the distance error ρ and the error in orientation ϕ for this run. We can see that ϕ is maintained close to zero and ρ is maintained around 5m on an average which equals $\rho_0 + R$. The oscillations may be caused by the GPS localization errors, which is on average 3m at Grand Isle. Thus Victoria tracks the curve successfully in the presence of real environmental disturbances and localization error.

Fig. 11 shows the AUV Fetch on a line following mission. The dotted line is the reference line Fetch 1 is trying to follow. The solid line shows the path taken by the Fetch. For this test, the two control gains used are: $\mu = 0.1$, $K_p = 0.001$ and the buffer is $\rho_0 = 8m$. The dynamics of the Fetch are notably slower than Victoria hence smoother convergence is observed in Fig. 11. In Fig. 12 we can see that Fetch 1 converges to the desired separation of $\rho_0 = 8m$ and ϕ stays close to zero. The oscillations caused by localization error still exist. This also shows that the control laws described in section III are robust even in the presence of winds, water currents, tides and engineering constraints such as sensor inaccuracy, localization errors, and network delays.

C. Cooperative control

Here we present results of our cooperative control experiments using ASV Victoria and Fetch 1. The goal of the experiment was to make the vehicles retain formation while tracking a line. Fig. 13 shows the result of our experiment. The vehicles were commanded to maintain a formation such that the y-coordinates of their position vectors coincide and a difference of $10m$ is maintained between the x-coordinates. We can see from Fig. 13 that the vehicles go away initially but in the end they come closer and their y-coordinates coincide whereas the separation in their x-coordinates is approximately $10m$. Also we can see that Fetch 1 is moving left towards the end. To maintain the difference in x-coordinates, Victoria tries to move in a conformable direction but it appears stuck/circling. It turns out that one of the thrusters of Victoria has failed and the experiments have to be canceled. We were not able to succeed in cooperatively tracking lines with two vehicles but the results showed in Fig.

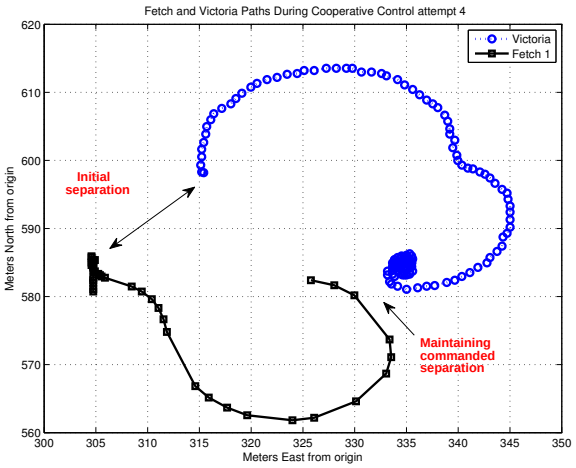

Fig. 13. A cooperative control experiment

13 are confirmation that our formation control algorithms were operational.

V. Conclusion and Future Work

We have presented experimental results evaluating the performance of controllers based on data collected during a 21 day survey performed at the Grand Isle, Louisiana. Our controllers have been tested on the Victoria class autonomous surface vessel (ASV-Victoria) and a Fetch class Autonomous Underwater Vehicle (AUV-Fetch). We have presented the experimental results of parameter identification, path following control, and formation control for two marine robots. We have shown that the control laws are robust even in the presence of natural disturbances like wind, water currents and engineering constraints such as sensor inaccuracy, localization errors, and network delays. With the help of a fleet of marine robots, we have collected large amounts of data to evaluate the level of reminiscent oil in the area after the Deepwater Horizon oil spill. The experimental work will be continued in summer 2012 where more experiments on formation control will be performed.

Acknowledgement

We would like to thank Prof. Mark Patterson's team from the College of William & Mary for supporting the operation of the Fetch. We would like to acknowledge, Prof. Michael Malisoff from the Department of Mathematics at Louisiana State University (LSU) for guidance on the robustness of the curve tracking control law, and Prof. Edward Overton of LSU for analyzing our water samples. We thank the Grand Isle State Park for support in field experiments. We express gratitude to Phillip Cheng and Brian Redden for their great work during the experiments. The research work is supported by NSF RAPID Grant ECCS-1056253, with partial support from: ONR grants N00014-08-1-1007, N00014-09-1-1074, and N00014-10-10712(YIP), and NSF grants ECCS-0845333(CAREER) and CNS-0931576. We have also received support from School of Electrical and Computer Engineering of Georgia Tech, from Georgia Tech Savannah Campus, and from other sponsors listed at http://gtsr.gtsav.gatech.edu/sponsors.

References

[1] "Deep Water: The Gulf Oil Disaster and the Future of Offshore Drilling - The Report of the National Commission on the BP Deepwater Horizon Oil Spill and Offshore Drilling," Jan 2011.

[2] K. Pettersen and O. Egeland, "Exponential stabilization of an underactuated surface vessel," in *Proceedings of the 35th IEEE Conference on Decision and Control*, vol. 1, 1996, pp. 967–972.

[3] K. Pettersen and E. Lefeber, "Way-point tracking control of ships," in *Proceedings of the 40th IEEE Conference on Decision and Control*, vol. 1, 2001, pp. 940–945.

[4] K. Do, Z. Jiang, and J. Pan, "Universal controllers for stabilization and tracking of underactuated ships," *Systems & Control Letters*, vol. 47, no. 4, pp. 299–317, Nov 2002.

[5] M. Breivik and T. Fossen, "Path following for marine surface vessels," in *OCEANS 2004*, vol. 4, Nov. 2004, pp. 2282–2289.

[6] M. Breivik, V. E. Hovstein, and T. I. Fossen, "Straight-Line Target Tracking for Unmanned Surface Vehicles," *Modeling, Identification and Control*, vol. 29, no. 4, pp. 131–149, 2008.

[7] I. Ihle, J. Jouffroy, and T. Fossen, "Formation control of marine surface craft: A Lagrangian approach," *IEEE Journal of Oceanic Engineering*, vol. 31, no. 4, pp. 922–934, 2006.

[8] H. Yang and F. Zhang, "Robust Control of Formation Dynamics for Autonomous Underwater Vehicles in Horizontal Plane," *ASME Journal of Dynamic Systems, Measurement and Control*, vol. 134, no. 3, p. 031009 (7 pages), 2011.

[9] K. Do and J. Pan, "Robust path following of underactuated ships using Serret-Frenet frame," in *Proceedings of the American Control Conference*, vol. 3, 2003, pp. 2000–2005.

[10] M. Malisoff, F. Mazenc, and F. Zhang, "Stability and Robustness Analysis for Curve Tracking Control using Input-to-State Stability," *IEEE Transactions on Automatic Control*, vol. 57, no. 5, pp. 1320–1326, 2011.

[11] K. Pettersen and T. Fossen, "Underactuated dynamic positioning of a ship-experimental results," *IEEE Transactions on Control Systems Technology*, vol. 8, no. 5, pp. 856–863, 2000.

[12] F. Zhang, E. Justh, and P. S. Krishnaprasad, "Boundary Following using Gyroscopic Control," in *Proceedings of the 43rd IEEE Conference on Decision and Control*, vol. 5, 2004, pp. 5204–5209.

[13] F. Zhang, D. M. Fratantoni, D. Paley, J. Lund, and N. E. Leonard, "Control of Coordinated Patterns for Ocean Sampling," *International Journal of Control*, vol. 80, no. 7, pp. 1186–1199, 2007.

[14] F. Zhang, A. O'Connor, D. Luebke, and P. S. Krishnaprasad, "Experimental Study of Curvature-based Control Laws for Obstacle Avoidance," in *Proceedings of 2004 IEEE International Conf. on Robotics and Automation*, vol. 4, 2004, pp. 3849–3854.

[15] M. Caccia, R. Bono, G. Bruzzone, E. Spirandelli, G. Veruggio, A. M. Stortini, and G. Capodaglio, "An Autonomous Craft for the Study of Sea-Air Interactions," *IEEE Robotics & Automation Magazine*, vol. 12, no. 3, pp. 95–105, 2005.

[16] J. Alves, P. Oliveira, and R. Oliveira, "Vehicle and mission control of the DELFIM autonomous surface craft," in *14th Mediterranean Conference on Control and Automation*, 2006, pp. 1–6.

[17] J. Manley, "Unmanned surface vehicles, 15 years of development," in *OCEANS 2008*, 2008, pp. 1–4.

[18] H. Ferreira, C. Almeida, A. Martins, J. Almeida, N. Dias, A. Dias, and E. Silva, "Autonomous bathymetry for risk assessment with ROAZ robotic surface vehicle," in *OCEANS 2009-Europe*, 2009, pp. 1–6.

[19] F. Zhang, "Geometric Cooperative Control of Particle Formations," *IEEE Transactions on Automatic Control*, vol. 55, no. 3, pp. 800–803, 2010.

[20] F. Zhang and N. E. Leonard, "Cooperative Control and Filtering for Cooperative Exploration," *IEEE Transactions on Automatic Control*, vol. 55, no. 3, pp. 650–663, 2010.

[21] ——, "Coordinated Patterns of Unit Speed Particles on a Closed Curve," *Systems and Control Letters*, vol. 56, no. 6, pp. 397–407, 2007.